Spectral-Based Group Formation Control

Shigeo Takahashi[1], Kenichi Yoshida[1], Taesoo Kwon[2], Kang Hoon Lee[3], Jehee Lee[2], and Sung Yong Shin[4]

[1]The University of Tokyo, Japan
[2]Seoul National University, Korea
[3]Kwangwoon University, Korea
[4]Korea Advanced Institute of Science and Technology, Korea

Abstract
Given a pair of keyframe formations for a group consisting of multiple individuals, we present a spectral-based approach to smoothly transforming a source group formation into a target formation while respecting the clusters of the involved individuals. The proposed method provides an effective means for controlling the macroscopic spatiotemporal arrangement of individuals for applications such as expressive formations in mass performances and tactical formations in team sports. Our main idea is to formulate this problem as rotation interpolation of the eigenbases for the Laplacian matrices, each of which represents how the individuals are clustered in a given keyframe formation. A stream of time-varying formations is controlled by editing the underlying adjacency relationships among individuals as well as their spatial positions at each keyframe, and interpolating the keyframe formations while producing plausible collective behaviors over a period of time. An interactive system of editing existing group behaviors in a hierarchical fashion has been implemented to provide flexible formation control of large crowds.

Categories and Subject Descriptors (according to ACM CCS): I.3.7 [Computer Graphics]: Three-Dimensional Graphics and Realism—Animation

1. Introduction

Many technical advancements have been made for intricate crowd control especially in the background scenes of movies and video games. Nonetheless, the full control of such crowds is still difficult because it requires appropriate parameters that faithfully characterize the crowd behaviors. On the other hand, in many cases, streams of crowd motions exhibit some meaningful formations such as artistic layouts in mass performances and tactical arrangements of players in team sports. To achieve this, the individuals try to get to their predefined positions at specific times while respecting their underlying collective movements.

In mass performances, for example, each individual is requested to keep a similar relative position with his/her neighbors while making smooth transitions between formations at predefined time steps. In this respect, the adjacency relationships should reflect the collective movement of the individuals, through which not only pleasing regular (but not random) patterns but also artistic expressiveness is exhibited to the audience according to a scenario.

This paper presents a novel approach to group formation control while maximally respecting the adjacency relationships among the involved individuals. Our main contribution lies in the use of *spectral analysis* of such clusters of individuals for plausible interpolation of the predefined keyframe formations.

A major advantage of our approach is the ability to control the adjacency relationship between any pair of individuals to maximally respect the underlying subgroups of individuals. Figure 9 shows that our approach achieves smooth changes in the spatial arrangements of subgroups, while the individuals in each subgroup are closely tied together during the motion. This advantage cannot be realized with geometric morphing techniques due to their limited capabilities of preserving the adjacency relationships. It is also difficult, if not impossible, with conventional *rule-based* approaches (for example, see [Rey99]) or *force-field-based* approaches (for example, see [HM95, GKM*01]) since a large number of parameters would have to be set properly to make these approaches work as intended.
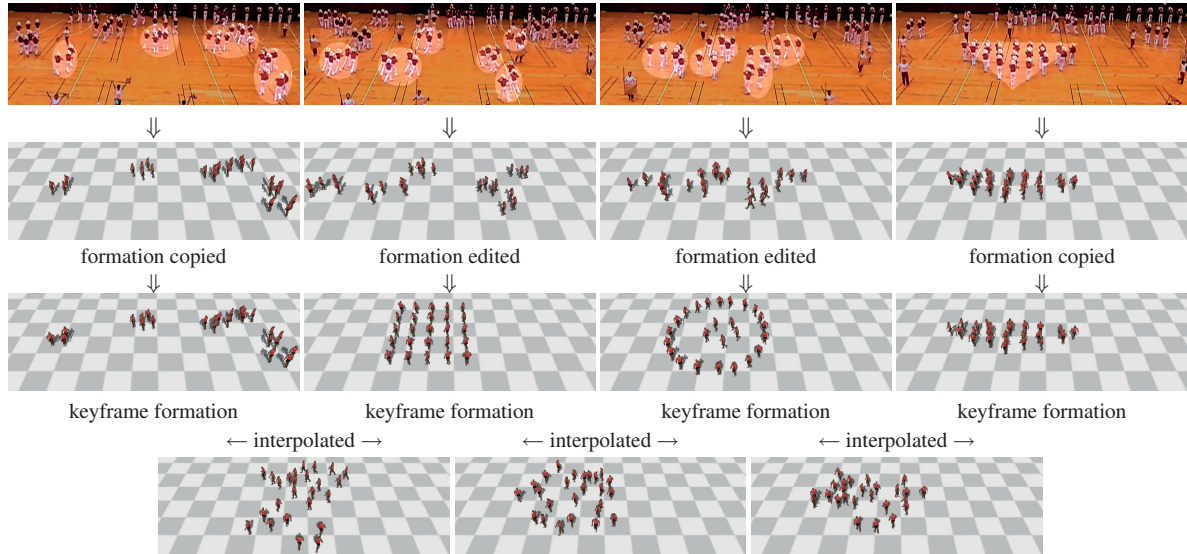
Figure 1: *Group formations in a mass performance of a marching band: A new sequence of group formations (in the bottom row) is generated from the video frames (in the top row) by extracting parts of the group formations (in the middle row), editing representative keyframe formations, and interpolating the formations for intermediate frames while respecting their adjacency.*

Another important advantage of our approach is that a stream of novel formations can be synthesized efficiently by minimally editing existing group formations, which can be readily acquired from various sources such as captured videos. Figure 1 illustrates the overview of this synthesis process, where the extracted group motion is edited by modifying certain representative keyframe formations and interpolating the corresponding relative arrangements to compose a novel sequence of group formations. This keyframe-based framework is suitable again in the design of mass performances, in which a scenario is usually provided beforehand by an artist so as to outline the sequence of representative formations with the underlying aggregate behaviors.

Our analysis for group formation is based on the *spectral graph theory* [Chu97], which allows us to partition a weighted graph with the minimal cost of edge cuts for clustering purposes. Here, a weighted graph is defined over a given group formation so that an edge weight represents the stability of the spatial adjacency between a pair of individuals. Spatial adjacencies are then captured by a *Laplacian matrix* to maximally respect the underlying local flocking behaviors of individuals in the group. Smooth interpolation over a sequence of given keyframe formations is achieved by successively transforming the *eigenstructures* of the Laplacian matrices. Hierarchical editing enables efficient control of a large crowd in our framework by recursively decomposing the crowd into several small subgroups of individuals. A social force model [HM95] is also integrated into the present approach in order to avoid collisions between the individuals during the interpolation of group formations.

The remainder of this paper is organized as follows: Section 2 surveys previous work related to this paper. Section 3 presents a new spectral-based method for smoothly interpolating keyframe formations, while trying to respect the underlying adjacency relationships among the individuals. Section 4 describes several enhancements of the present approach for better control of group formations. After demonstrating crowd animation results together with the implementation of our prototype system in Section 5, Section 6 concludes this paper and refers to possible future extensions.

2. Related Work

Conventional methods for crowd behavioral control can be roughly classified into *microscopic* and *macroscopic* approaches, where a microscopic approach describes the local motion of each individual in a crowd while a macroscopic approach tries to govern the global behavior of the crowd.

The most popular are *rule-based* approaches in which microscopic rules are defined for autonomous agents. Reynolds [Rey99] simulated flocks of birds and schools of fishes using simple local behavioral rules, where the approach was equipped with a steering behavior to make the individuals reach their goals while avoiding obstacles and collisions with others. Rule-based models have been more sophisticated by accounting for motion dynamics [BH97], cognitive knowledge [FTT99], human psychology [SMK05], pedestrian perception [ST05], and densely populated situations [PAB07].

On the other hand, different approaches have been intro-

duced to govern such behaviors of crowds with the help of *force-field* formulations. *Social forces* introduced by Helbing and Molnár [HM95] are an example of such physical forces, and can systematically regulate mutual microscopic interactions between individuals in escape panic [BMdB03] and pedestrian simulation [LKF05].

Different physical sophistication, originated from *fluid dynamics*, has then been invented to explore rather macroscopic behavior of crowds. This class of methods has enabled the global configuration of obstacles with vector fields [GKM*01], and pedestrian behavioral control with continuous density fields [Hug03, TCP06]. An alternative approach is presented to design a stationary flow field by manually tiling small rectangular regions of velocity fields over the environment [Che04].

Although these methods effectively simulate the realistic behavior of crowds, they still incur unexpected artifacts in the motion of each agent due to interactions with other moving agents. *Example-based* models solve this problem by referring to the existing motion data and synthesize naturally-looking crowd animations, including rhythmic motions such as ballroom dancing and military marching [KPS03] and composite motion of existing group behaviors using extended motion graphs [SKG05, LCF05]. Recently, several methods have been proposed that directly use videos of real crowds rather than motion capture data, where the existing crowd motions are extracted manually [LCL07, PPD07] and semi-automatically [LCHL07, CC07] from the videos.

Our approach can be categorized into a macroscopic approach, however, its goal is somewhat different from the conventional approaches of the same kind in that it explores explicit control of spatial adjacencies between individuals or their subgroups rather in unconstrained environments, in order to generate meaningful spatiotemporal transitions as exhibited in mass performances and tactical sports. Such group formation control has been investigated in the field of robotics [LT97, BA98, LC03], while the methods cannot provide smooth transitions of global group formations. On the other hand, our approach employs spectral analysis of adjacency relationships among individuals for sophisticated control of the underlying aggregate behaviors. This spectral analysis technique is also closely related to graph layout problems [Kor03], and thus can be extended to the analysis of point sets such as clustering [SM00] and matching [CH03]. Furthermore, the spectral-based approach is suitable for mesh manipulations such as smoothing [Tau95], compression [KG00], and watermarking [OMT02]. A similar idea has been recently employed for the global deformation of group pathways while their details are maintained [KLLT08]. We refer the reader to the book [Chu97] for more details.

3. Spectral Formation Control

This section explains fundamentals of our spectral-based approach to group formation control using adjacency relationships among individuals. Our strategy is to extract *adjacency relationships* from coarse to fine frequencies, and interpolate them for each frequency to preserve the collective behaviors of individuals.

3.1. Formation analysis

First of all, we associate a graph with a group formation in order to describe the adjacency relationships among individuals. Figure 2(a) shows an example of a graph that represents the adjacency relationships among six individuals. A vertex of the graph represents an individual. Let n be the number of individuals in a group. Each edge connecting vertices i and j, for $1 \leq i, j \leq n$ and $i \neq j$, has a positive weight w_{ij}, where $w_{ij} = w_{ji}$. Basically, the weight value represents the stability of the corresponding adjacency relationship during the spatiotemporal transition of the group formation. Notice that not every pair of vertices admits an edge. By default, we use the *Delaunay triangulation* of the vertices as the graph, and set each edge weight w_{ij} to the inverse of the distance between vertices i and j. However, the connectivity of the graph and its associated edge weights can be modified arbitrarily in formation editing, regardless of their spatial arrangement. In order to extract the spectral-based structure of a group formation, we analyze the $n \times n$ *Laplacian matrix L* of the graph, which is defined as follows [Kor03]:

$$L = (L_{ij}) = \begin{cases} \sum_{m=1}^{n} w_{im} & i = j \\ -w_{ij} & i \neq j \end{cases}, \quad i, j = 1, \ldots, n.$$

Figure 2 (b) shows a Laplacian matrix, where all the edges of the graph have a unit weight value for simplicity. Since L is always a symmetric positive definite matrix, the eigenvalues are all nonnegative and its corresponding unit eigenvectors form an n-dimensional *orthonormal basis* called an *eigenbasis*. In particular, the minimum eigenvalue of L is always 0 and its corresponding eigenvector is $(1, \ldots, 1)$ since the sum of the matrix entries in each row vanishes.

The eigenanalysis of L allows us to decompose the graph structure into its frequency components [KG00]. Let $0 = \lambda_1 \leq \lambda_2 \leq \cdots \leq \lambda_n$ be the eigenvalues of L, and $e_1, e_2, \ldots,$ and e_n their corresponding unit eigenvectors. Denoting the 2D coordinates of the individual k by $(x_k, y_k), k = 1, \ldots, n$, we define two column vectors of dimension n: $x = (x_1, \ldots, x_n)^\top$ and $y = (y_1, \ldots, y_n)^\top$, where $\top$ denotes the transpose of a vector. These column vectors can be written as a weighted sum of the eigenvectors as:

$$x = \alpha_1 e_1 + \cdots + \alpha_n e_n \quad \text{and} \quad y = \beta_1 e_1 + \cdots + \beta_n e_n. \quad (1)$$

Here α_k and β_k are coefficients satisfying $\alpha_k = \langle x, e_k \rangle$ and $\beta_k = \langle y, e_k \rangle$, respectively, where $\langle p, q \rangle$ is the inner product of vectors p and q. Figure 2(c) illustrates such a frequency-based decomposition of the graph in Figure 2(a), where the
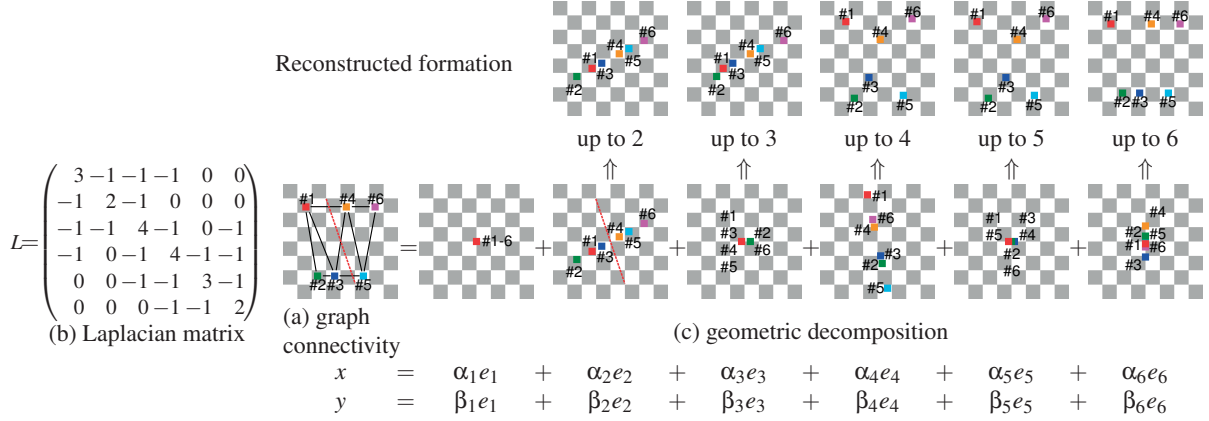
Reconstructed formation

up to 2   up to 3   up to 4   up to 5   up to 6

$$L=\begin{pmatrix} 3 & -1 & -1 & -1 & 0 & 0 \\ -1 & 2 & -1 & 0 & 0 & 0 \\ -1 & -1 & 4 & -1 & 0 & -1 \\ -1 & 0 & -1 & 4 & -1 & -1 \\ 0 & 0 & -1 & -1 & 3 & -1 \\ 0 & 0 & 0 & -1 & -1 & 2 \end{pmatrix}$$

(b) Laplacian matrix

(a) graph connectivity

(c) geometric decomposition

$$x = \alpha_1 e_1 + \alpha_2 e_2 + \alpha_3 e_3 + \alpha_4 e_4 + \alpha_5 e_5 + \alpha_6 e_6$$
$$y = \beta_1 e_1 + \beta_2 e_2 + \beta_3 e_3 + \beta_4 e_4 + \beta_5 e_5 + \beta_6 e_6$$

Figure 2: *Graph decomposition using spectral analysis: (a) original graph connectivity (center), (b) its corresponding Laplacian matrix (left), and (c) geometric decomposition (right). The eigenvector e_1 relates to the barycenter of the graph, the eigenvectors e_2–e_6 represent how the individuals can be clustered into subgroups from coarse to fine levels. The original formation can be reconstructed by accumulating the components from coarse to fine frequencies, accordingly.*

eigenvector e_k gives rise to the arrangement of the individuals along the direction vector $(\alpha_k, \beta_k)^\top$. Moreover, the eigenvector for a smaller eigenvalue controls larger clusters of individuals in the group formation, except that e_1 just relates to the barycenter of the group because $e_1 = \frac{1}{n}(1,\ldots,1)^\top$. For example, we can bisect the graph only with 3 edge cuts with respect to $(\alpha_2, \beta_2)^\top$ in this case as indicated by red broken lines; otherwise we would need 4 or more edge cuts.

3.2. Formation interpolation

Having extracted the Laplacian matrices for the source and target keyframe formations, our task is to smoothly interpolate the two keyframe formations while achieving their plausible transition. We separately interpolate the eigenbases of the Laplacian matrices and their associated coefficient vectors (See Eq. (1)), which correspond to the adjacency relationships among individuals and their geometric positions in 3D space, respectively, in a mathematical sense.

Given a pair of Laplacian matrices corresponding to the source and target group formations, respectively, element-wise linear interpolations would not properly reflect the given adjacency relationships of the group, unfortunately. At every time step during a formation transition, the unit eigenvectors of the Laplacian matrix form an orthonormal basis because the Laplacian matrix is always a symmetric positive definite matrix as described earlier. This observation inspires us to perform formation control by transforming the eigenvectors of the Laplacian matrix for the source group formation into the target eigenvectors, while keeping their orthonormality during the transformation. Rotation is the transformation of our choice as it is the only transforma-

tion that satisfies this orthonormality condition while being simple and natural.

Let $\lambda_k^S, k = 1,\ldots,n$ be the eigenvalues of the Laplacian matrix for the source group formation such that $0 = \lambda_1^S \leq \cdots \leq \lambda_n^S$, and e_k^S be the corresponding eigenvectors. Similarly, we define the eigenvalues and eigenvectors of the target formation as λ_k^T and $e_k^T, k = 1,\ldots,n$. Letting $S = (e_1^S,\ldots,e_n^S)$ and $T = (e_1^T,\ldots,e_n^T)$, we derive an $n \times n$ rotation matrix R as follows:

$$R = T S^{-1}. \tag{2}$$

This formulation also takes into account the eigenvalues (i.e., the frequency) of the Laplacian matrix by arranging the eigenvectors in S and T according to the magnitudes of the corresponding eigenvalues, respectively. Without loss of generality suppose that $\det(S) = \det(T) = 1$ and $\langle e_k^S, e_k^T \rangle \geq 0$. These conditions can always be achieved by properly inverting the direction of $e_k^T, k = 1,\ldots,n$, if needed. This arrangement of eigenvectors enables us to not only retain the aggregation of individuals in the group formation, but also to smoothly merge and split existing clusters by changing the associated adjacencies.

Let us denote the $n \times n$ matrix of eigenvectors at the time t by $M(t) = (e_1(t), e_2(t),\ldots,e_n(t))$. For the actual formation interpolation, the rotation matrix $R^t, t \in [0,1]$ gives us the matrix $M(t)$ as follows:

$$M(t) = R^t S. \tag{3}$$

A more sophisticated scheme for eigenvector ordering is to be discussed in Section 4.2. The actual computation for the exponential of the matrix R will be detailed in Section 5.
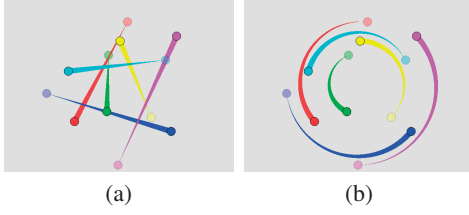
(a)   (b)

Figure 3: *Differences between (a) linear interpolation and (b) polar interpolation where the associated relative arrangement remains the same.*
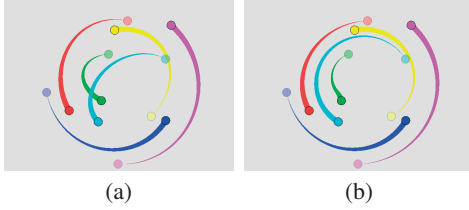

(a)   (b)

Figure 4: *Differences between formation transitions (a) without the PCA-based adjustment and (b) with the PCA-based adjustment, where the associated relative arrangements in the source and target formations are not identical. The green and cyan trajectories intersect without the PCA-based adjustment while the relative arrangement is maximally preserved with the PCA-based adjustment.*

3.3. Geometric interpolation

On top of formation interpolation, we also perform geometric interpolation to fix the coefficient vectors at each time step. Since Eq. (3) provides the eigenvectors $e_1(t), \ldots, e_n(t)$ at the time t, we can determine the (x,y)-coordinates of each individual using Eq. (1), given coefficients $\alpha_k(t)$ and $\beta_k(t)$, $k = 1, \ldots, n$. We obtain these coefficients based on *polar interpolation* in 3D space over the time interval $[0,1]$.

Probably the simplest method to obtain the coefficients may be linear interpolation between source coefficients $(\alpha_k^S, \beta_k^S)^\top$ and target coefficients $(\alpha_k^T, \beta_k^T)^\top$. Unfortunately, such a method is not able to respect the adjacency relationships among individuals even when the two group formations share the same relative arrangement, as illustrated in Figure 3(a). In this figure, a different color is assigned to each individual in order to represent its own source position, target position, and trajectory between them with a translucent disk, an opaque disk, and a curved line with increasing thickness, respectively. Note that the barycenter of the formation remains fixed during the transformation in this case. This observation motivates the use of polar interpolation in order to align the orientation of the source formation with that of the target formation during the interpolation, as shown in Figure 3(b). Our polar interpolation scheme can be
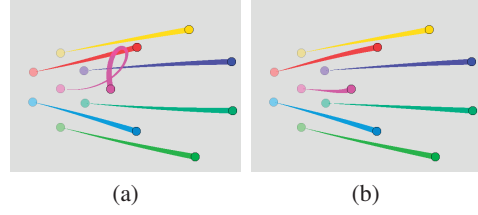

(a)   (b)

Figure 5: *Formation transitions obtained with (a) simple polar interpolation, and (b) our spectral-based interpolation. The PCA-based adjustment is applied to both cases.*

formulated as follows:

$$\begin{pmatrix} \alpha_k(t) \\ \beta_k(t) \end{pmatrix} = \begin{pmatrix} r_k(t)\cos(\theta_k(t)) \\ r_k(t)\sin(\theta_k(t)) \end{pmatrix}, \text{ where } \begin{array}{l} r_k(t) = (1-t)r_k^S + tr_k^T, \\ \theta_k(t) = (1-t)\theta_k^S + t\theta_k^T, \end{array}$$

$$r_k^S = \left| \begin{pmatrix} \alpha_k^S \\ \beta_k^S \end{pmatrix} \right|, r_k^T = \left| \begin{pmatrix} \alpha_k^T \\ \beta_k^T \end{pmatrix} \right|, \theta_k^S = \text{atan}\begin{pmatrix} \alpha_k^S \\ \beta_k^S \end{pmatrix}, \text{ and } \theta_k^T = \text{atan}\begin{pmatrix} \alpha_k^T \\ \beta_k^T \end{pmatrix}. \quad (4)$$

Here, $r = |(\alpha, \beta)^\top|$ represents the norm of the vector $(\alpha, \beta)^\top$, and atan $(\alpha, \beta)^\top$ denotes the angle between the vectors $(\alpha, \beta)^\top$ and $(1,0)$. Note that, for $k = 0$, we employ linear interpolation because the corresponding coefficients just represents the barycenters of the two formations.

This polar interpolation scheme is also advantageous even if the two given formations are moderately different. In this case, special care is needed to minimize the change in the relative arrangement during the formation transition. Without loss of generality, suppose that the source and target formations are translated to share the barycenter. We first find the principal axes of the two formations from their spatial arrangements using principal component analysis (PCA), and then rotate the target formation until their principal axes are aligned with those of the source formation. We call this the *PCA-based adjustment* of group formations in this paper.

After this PCA-based adjustment, we carry out the polar interpolation described above (See Eq. (4)). For each individual, there are two rotation directions, that is, clockwise and counter-clockwise directions. We choose the direction that yields the smallest rotation angle. Figure 4 shows how the PCA-based adjustment maximally preserves the relative positions of individuals during the interpolation, by switching the rotation directions of individuals in green and cyan.

Let us compare our spectral-based interpolation with *simple polar interpolation* where we directly interpolate the positions of each individual using these polar coordinates, without decomposing them into spectral coefficients as in Eq. (1). Our spectral-based approach is more effective than simple polar interpolation, since it maximally respects the spatial adjacency among the individuals as shown in Figure 5. Note that with simple polar interpolation we can see an unexpected winding path for the individual in magenta.
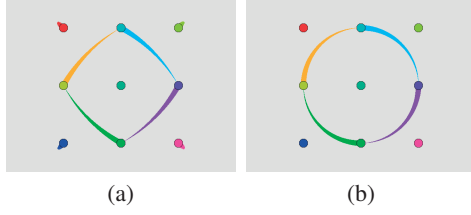
As described in Section 3.1, another advantage of our

(a)   (b)

Figure 6: *Formation transitions obtained with (a) adjacency relationships based on the spatial arrangement of individuals and (b) with adjacency relationships manually adjusted.*
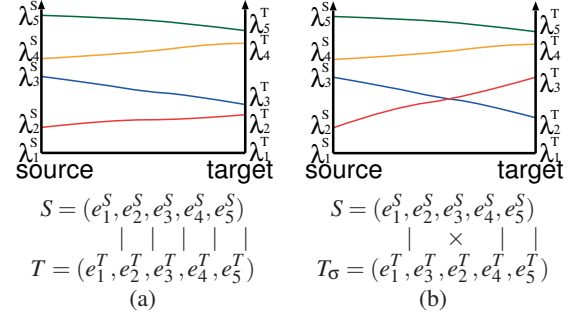

(a)   (b)

Figure 7: *Reordering eigenvectors for fine adjustment of source and target orthonormal bases: (a) transitions of eigenvalues when the group formation has a small change and (b) when the formation has a relatively large change. The matrices of reordered eigenvectors for source and target formations are represented at the bottom.*
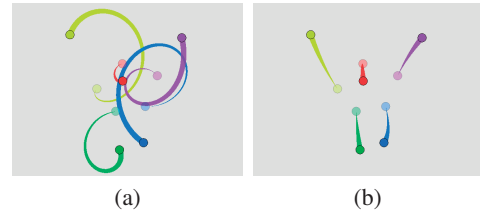
approach is the ability to control the stability of the adjacency relationships during the associated spatiotemporal transition. Figure 6 shows comparison between two formation transitions with the edge weights derived from the purely-geometric setting of the individuals (Figure 6(a)) and with edge weights manually adjusted (Figure 6(b)). In Figure 6(b), we tightly control the relative positions of the four moving individuals and the central one by manually increasing each of the corresponding edge weights by ten times, compared to that in Figure 6(a).

4. Enhancement of Formation Control

In this section we describe several enhancements of the proposed framework for better control of formation transition, to take full advantage of the fundamentals presented in the previous section.

4.1. Interpolating multiple formations

Interpolating more than two keyframe formations is important in the present framework to allow users to insert new intermediate keyframe formations. We solve the problem by extending the *Catmull-Rom spline* formulation [CR74]. Provided with control points p_{n-1}, p_n, p_{n+1}, and p_{n+2}, a Catmull-Rom spline curve that begins at p_n and ends at p_{n+1} is defined as:

$$p(t) = c_{-1}p_{n-1} + c_0p_n + c_1p_{n+1} + c_2p_{n+2}, \text{ where}$$
$$c_{-1} = \tau(-t + 2t^2 - t^3), \quad c_0 = (1 - 3t^2 + 2t^3) + \tau(t^2 - t^3) \quad (5)$$
$$c_1 = (3t^2 - 2t^3) + \tau(t - 2t^2 + t^3), \text{ and } c_2 = \tau(-t^2 + t^3).$$

Here, $t \in [0, 1]$ and τ control the tension of the curve. In our implementation, we set $\tau = 0.5$ by default. In addition, when p_n (or p_{n+1}) is an endpoint of the curve, or a point at which the curve is set to be nonsmooth, p_n (or p_{n+1}) is duplicated.

For finding the temporal transition of the matrix of eigenvectors $M(t)$ in Eq. (3), let R_0, R_1, and R_2 be the three rotation matrices that successively transform the given keyframe formation represented by the matrix of eigenvectors M_0. Applying the spline formulation to the power of rotation matri-

(a)   (b)

Figure 8: *Paths of the individuals without and with eigenvector reordering: (a) winding paths without eigenvector reordering and (b) smooth paths with eigenvector reordering.*

ces will give us the following equation:

$$\begin{aligned}
M(t) &= (R_2R_1R_0)^{c_2}(R_1R_0)^{c_1}(R_0)^{c_0}(I)^{c_{-1}}M_0 \\
&= (R_2R_1R_0)^{c_2}(R_1R_0)^{c_1}(R_0)^{c_0}M_0,
\end{aligned}$$

where c_{-1}, c_0, c_1, and c_2 are defined in Eq. (5), and I represents the identity matrix. This formulation enables smooth interpolation of adjacency relationships among individuals over the given multiple keyframe formations.

4.2. Eigenvector reordering

Ordering the eigenvectors of the Laplacian matrix according to their corresponding eigenvalues yields a natural transition between a pair of keyframe formations when the two formations share moderately similar spatial adjacencies among the individuals. This follows from the fact that, in such a case, the order of eigenvalues usually remains the same over the period of time as shown in Figure 7(a), except for the first eigenvalues representing the formation barycenter. Nonetheless, this scheme sometimes incurs unexpected path winding for individuals, as shown in Figure 8(a), if the two given formations are relatively different in their adjacency relationships. This problem occurs when the associated order of the

eigenvalues has changed during the transition as shown in Figure 7(b).

In our approach, we alleviate this problem by reordering the eigenvectors of the keyframe formations by greedy pairwise coupling. This reordering is accomplished, as shown in Figure 7(b), by first fixing the order of source eigenvectors $(e_2^S, \ldots, e_n^S)$, and then finding the new order of target eigenvectors $(e_{\sigma(2)}^T, \ldots, e_{\sigma(n)}^T)$ such that the corresponding inner product $\langle e_k^S, e_{\sigma(k)}^T \rangle$ is maximized. More precisely, for each source eigenvector $e_k^S, k = 2, \ldots, n$, $e_{\sigma(k)}^T$ is chosen successively among the uncoupled target eigenvectors from $k = 2$ to n in a greedy manner. The resultant reordering of target eigenvectors usually provides smoother paths because the target orthonormal basis is now closely aligned to the source orthonormal basis. Figure 8(b) shows an effect of this reordering where the undesirable path winding has been successfully eliminated. Our framework also provides an option for further improving this alignment, by locally rearranging the target eigenvectors in order to maximize the minimum inner product (i.e., minimize the maximum angle between the corresponding eigenvectors) over all the combinations of corresponding source and target eigenvectors.

4.3. Collision avoidance

As described so far, our approach ignores potential collisions between individuals. A social force model [HM95] is integrated into our approach for collision avoidance. We first generate the trajectory of each individual using our macroscopic spectral-based approach. We then locally adjust this trajectory by applying social forces such as driving and repulsive forces to avoid collisions. We finally smooth the trajectory while keeping a user-specified minimum interdistance for every pair of individuals. Figure 9 shows how this process successfully generates collision-free trajectories for interpolating group formations. The comparison with the simple social force model reveals that our approach provides more plausible macroscopic transitions as initial trajectories and is also naturally compatible with existing microscopic path generation frameworks using social forces. Note that this collision-avoidance scheme is similar to Perlin's work [Per].

4.4. Hierarchical control

In order to handle a crowd consisting of a large number of individuals, we take a divide-and-conquer strategy to decompose the crowd into subgroups of individuals, each of which shares a common goal. This motivates the use of a *hierarchical representation* for crowd control [MT01], with which we can recursively describe the behaviors of a large crowd in terms of subgroups. In particular, the spectral-based approach is applied to the subgroups at each level from top to bottom in a hierarchical fashion. The position of each subgroup is set to the barycenter of the individuals in the sub-
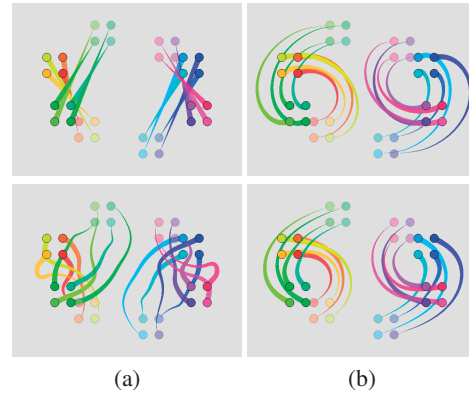

(a)   (b)

Figure 9: *Comparison between (a) linear and (b) spectral-based interpolation schemes. Original macroscopic trajectories as initial solutions (top) and those obtained by collision avoidance using social forces (bottom). Our spectral-based macroscopic interpolation maximally preserves the underlying clusters of individuals, and is also compatible with existing microscopic behavioral control of individuals.*

group. The hierarchical control scheme facilitates a systematic way of handling meaningful crowd formations, such as simulating a large crowd in specific formations (Figure 11).

4.5. Extension to 3D cases

Our approach can be extended to control 3D group formations such as flocks of birds and schools of fishes. We straightforwardly adapt the two-step approach in 2D space that consists of formation interpolation (Section 3.2) and geometric interpolation (Section 3.3). For geometric interpolation, we employ a *spherical linear interpolation* technique [Sho85]. Figure 12 presents an airshow scene generated using our approach where airplanes exhibit acrobatic changes of formations in 3D space.

5. Results

This section describes an implementation of our prototype system for group formation control, and demonstrates several animation results generated by the system in order to illustrate the capability of our approach. Discussions of the advantages and limitations of the present approach are also provided. See the accompanying video for details.

5.1. Editing interface

Our prototype system is implemented on a desktop PC with an Intel Core 2 Duo E6600 CPU (2.4GHz, 4MB cache) and 3GB RAM. The prototype system allows the user to freely edit keyframe formations to facilitate intended group formation control at an interactive rate. The interactive performance is accomplished by approximating the power of

Figure 10: *Tactical formations in a soccer game: (a) A keyframe when the offside trap is about to begin, (b) a keyframe when the offside trap fails, (c) a new keyframe when the offside trap is about to begin, and (d) a new keyframe when the offside trap is successful.*
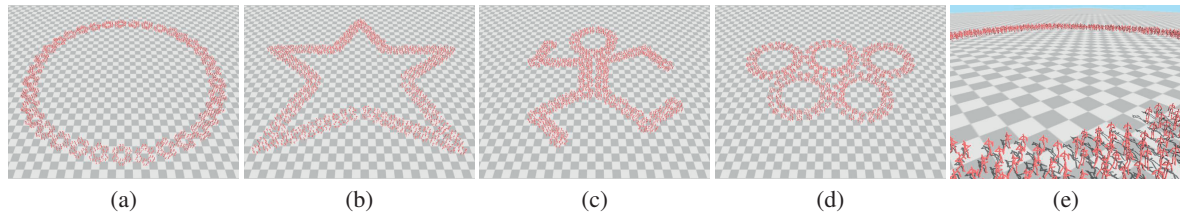

Figure 11: *Artistic formations in the mass performance of a large crowd. Four keyframe formations are inserted to guide the formation: (a) A circle, (b) a star, (c) a runner, (d) five small circles, and (e) a side view of the crowd.*

matrices using the method for computing matrix square roots [DB76]. The system also provides default setting of the adjacency relationships based on the vertex connectivity of the Delaunay triangulation, which will serve as a good starting point for further editing the adjacency relationships among individuals and their hierarchical representations.

5.2. Animation examples

We calculated the trajectory of each individual with the present approach, and used an online locomotion synthesis technique [KS07] as a postprocess to control human-like individuals in Figures 1, 10, and 11. Table 1 shows statistics of group formations in the animation examples, where the computation times were measured by conducting the above postprocess for the final motion synthesis.

Mass performance of a marching band Figure 1 presents how we can modify the existing motion in a mass performance done by a marching band. Here, we extracted the group motion from a video clip (in the top row) [LCHL07]. We then inserted two intermediate formations as new keyframes in addition to the first and last formations, intensified the adjacency relationships among individuals in each subgroup, and finally generated a novel sequence of group formations. A sequence of snapshots of the resulting animation is exhibited in the bottom two rows of Figure 1.

Soccer game Figure 10 demonstrates how to edit a tactical formation in a soccer game. In the original scene (Figure 10(b)), a defensive tactic called an offside trap is not

successful because the player in the defensive group is not properly placed (Figure 10(a)) when the ball is passed. Note that an offensive player commits an offside fault if the player is behind the last defensive players (except the goalkeeper) without keeping the ball. We can modify this scene to show that the defensive group achieves the intended offside trap (Figure 10(d)), by spatially aligning the last defenders on a line in a keyframe formation (Figure 10(c)).

Large crowd in specific formations Figure 11 demonstrates that our approach is also feasible for controlling a large number of individuals in a crowd. In this experiment, we introduced three hierarchical levels for representing the crowd, by recursively splitting it into disjoint subgroups and controlling their formations and local behaviors. The number of hierarchical levels was manually designed in this case, while the associated grouping could be conducted semi-automatically with the support of our system. We used four keyframe formations as shown in Figures 11(a)-(d).

Acrobatic airshow In order to demonstrate the capability of 3D group formation control, we show a synthetic animation of airplanes in Figure 12, successively exhibiting six alphabet characters "T," "H," "E," "E," "N," and "D." The airplanes move plausibly to interpolate these specified keyframes while respecting their adjacency relationships in 3D space.

5.3. Discussions

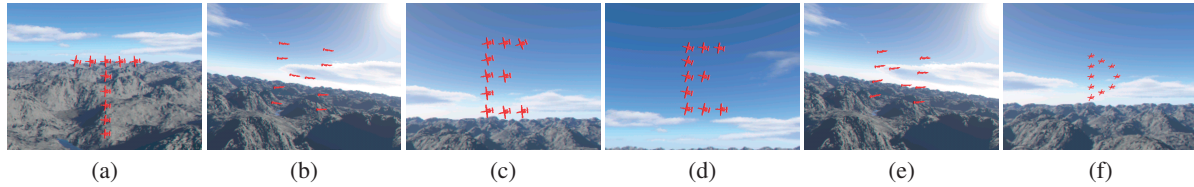Our approach aims at macroscopic control of group behaviors assuming that a group motion is prescribed as a series

| (a) | (b) | (c) | (d) | (e) | (f) |

Figure 12: *A sequence of acrobatic formations in an airshow: The letters (a) "T," (b) "H," (c) "E," (d) "E," (e) "N," and (f) "D," which are given as keyframe formations.*

of keyframe formations. In other words, our scheme is not intended to generate group motions that mainly depend on various microscopic interactions such as pedestrian behaviors and escape panic. To our knowledge, our approach is the first scheme for macroscopic formation control, which facilitates smooth transitions of keyframe formations and accurate spatiotemporal control of each individual at specific keyframes. In order to keep interactivity of our system, we limit the number of individuals up to 60 in a single subgroup; otherwise, the computation time for eigenanalysis (see Section 3) would increase rapidly. Applying different interpolation schemes such as linear and spectral-based interpolations and their blends to each pair of subgroups will enhance the expressive power of the formation transitions to be designed.

Our system specifies motions of individuals only by their time-parametrized trajectories. Thus, the control of local speed and moving style (walking or running) of each individual for realistic behavior, highly relies on a trajectory-driven motion synthesis scheme used in a postprocessing stage. However, the online locomotion synthesis employed here [KS07] can produce a visually-plausible behavior for each individual, provided that the temporal samples taken from the corresponding trajectory are almost uniformly spaced in 3D space, as demonstrated in Figures 1, 10, and 11. Although our approach focuses on formation control in unconstrained environments, handling static obstacles, such as houses and walls, also as graph vertices can allow us to simulate the specific clearance between the obstacles and individuals together with the appropriate setting of associated adjacency weights. More aggressive splitting and merging of formation clusters will simulate more natural collective behaviors of individuals as seen in flocks of birds and schools of fishes. This will be accomplished by appropriately controlling the adjacency weights between the subgroups at the same depth in the hierarchical representation of the overall formation.

6. Conclusion

This paper has presented an approach to group formation control using the spectral graph theory, based on the intuition that the adjacency relationships among the individuals play a significant role in group formations as observed in artistic formations of mass performances and the tactical formations of team sports. The main idea behind this approach is to extract the spectral-based structures of group formations, which is achieved through the Laplacian matrices of the graph associated with their adjacency relationships among individuals. The interpolation between group formations is obtained by rotational transformations of eigenbases for the Laplacian matrices in order to change the collective behaviors of individuals smoothly over time. Our spectral-based approach can be enhanced with several extended features. Animation results are generated to demonstrate the capabilities of the present approach.

Our future extensions include semi-automatic individual matching between multiple formations, which will be helpful for efficient design of group formation animation. It would be interesting to apply this approach to other problems such as the control of satellite constellations and animation of time-varying relationships in the context of information visualization. Controlling formations in environments with obstacles are also important potential applications of this approach. We also leave it as future work to enhance our framework by explicitly incorporating ideas from existing approaches including rule-based and force-field-based models.

References

[BA98] BALCH T., ARKIN R. C.: Behavior-based formation control for multirobot teams. *IEEE Trans. Robotics and Automation* *14* (1998), 926–939.

Table 1: *Statistics of the group formations in the animation examples.*

	# of levels	# of individuals	structure of the entire formation	# of frames	computation times (cf. [KS07])
Marching band	2	25	$= 3 + 5 + 5 + 5 + 4 + 3$ (6 groups)	1211	11 seconds
Soccer	2	14	$= 6$(offense) $+ 8$(defense) (2 groups)	238	14 seconds
Human figures	3	1260	$= 35$(groups) $\times 6$(subgroups) $\times 6$(individuals)	991	445 seconds
Airshow	1	10	$= 10$ (airplanes at one level)	540	NA (in real time)

[BH97] BROGAN D. C., HODGINS J. K.: Group behaviors for systems with significant dynamics. *Autonomous Robots 4* (1997), 137–153.

[BMdB03] BRAUN A., MUSSE S. R., DE OLIVEIRA L. P. L., BODMANN B. E. J.: Modeling individual behaviors in crowd simulation. In *Proc. Computer Animation and Social Agents 2003* (2003), pp. 143–148.

[CC07] COURTY N., CORPETTI T.: Crowd motion capture. *Computer Animation and Virtual Worlds 18* (2007), 361–370.

[CH03] CARCASSONI M., HANCOCK E. R.: Spectral correspondence for point pattern matching. *Pattern Recognition 36* (2003), 193–204.

[Che04] CHENNEY S.: Flow tiles. In *Proc. Symp. Computer Animation 2004* (2004), pp. 233–242.

[Chu97] CHUNG F. R. K.: *Spectral Graph Theory*. American Mathematical Society, 1997.

[CR74] CATMULL E., ROM R.: A class of local interpolating splines. In *Computer Aided Geometric Design*, Barnhill R. E., Reisenfeld R. F., (Eds.). Academic Press, 1974, pp. 317–326.

[DB76] DENMAN E. D., BEAVERS JR. A. N.: The matrix sign function and computations in systems. *Applied Mathematics and Computations 2* (1976), 63–94.

[FTT99] FUNGE J., TU X., TERZOPOULOS D.: Cognitive modeling: Knowledge, reasoning and planning for intelligent characters. In *Proc. Siggraph '99* (1999), pp. 29–38.

[GKM*01] GOLDENSTEIN S., KARAVELAS M., METAXAS D., GUIBAS L., AARON E., GOSWAMI A.: Scalable nonlinear dynamical systems for agent steering and crowd simulation. *Computers & Graphics 25* (2001), 983–998.

[HM95] HELBING D., MOLNÁR P.: Social force model for pedestrian dynamics. *Pysical Review E 51* (1995), 4282–4286.

[Hug03] HUGHES R. L.: The flow of human crowds. *Annual Review of Fluid Mechanics 35* (2003), 169–182.

[KG00] KARNI Z., GOTSMAN C.: Spectral compression of mesh geometry. In *Proc. Siggraph 2000* (2000), pp. 279–286.

[KLLT08] KWON T., LEE K. H., LEE J., TAKAHASHI S.: Group motion editing. *ACM Trans. Graphics 27* (2008). Article 80.

[Kor03] KOREN Y.: On spectral graph drawing. In *Proc. Int'l Computing and Combinatorics Conf. 2003 (LNCS 2697)* (2003), Springer-Verlag, pp. 496–508.

[KPS03] KIM T.-H., PARK S. I., SHIN S. Y.: Rhythmic-motion synthesis based on motion-beat analysis. *ACM Trans. Graphics 22* (2003), 392–401.

[KS07] KWON T., SHIN S. Y.: A steering model for on-line locomotion synthesis. *Computer Animation and Virtual Worlds 18*, 4-5 (2007), 463–472.

[LC03] LI T.-Y., CHOU H. C.: Motion planning for a crowd of robots. In *Proc. IEEE Int'l Conf. on Robotics and Automation 2003* (2003), pp. 4215–4221.

[LCF05] LAI Y., CHENNEY S., FAN S.: Group motion graphs. In *Proc. Symp. Computer Animation 2005* (2005), pp. 281–290.

[LCHL07] LEE K. H., CHOI M. G., HONG Q., LEE J.: Group behavior from video: A data-driven approach to crowd simulation. In *Proc. Symp. Computer Animation 2007* (2007), pp. 109–118.

[LCL07] LERNER A., CHRYSANTHOU Y., LISCHINSKI D.: Crowds by example. *Computer Graphics Forum 26* (2007), 655–664.

[LKF05] LAKOBA T. I., KAUP D. J., FINKELSTEIN N. M.: Modifications of the Helberg-Molnár-Farkas-Vicsek social force model for pedestrian evolution. *Simulation 81* (2005), 339–352.

[LT97] LEWIS M. A., TAN K.-H.: High precision formation control of mobile robots using virtual structures. *Autonomous Robots 4* (1997), 387–403.

[MT01] MUSSE S. R., THALMANN D.: Hierarchical model for real time simulation of virtual human crowds. *IEEE Trans. Visualization and Computer Graphics 7* (2001), 152–164.

[OMT02] OHBUCHI R., MUKAIYAMA A., TAKAHASHI S.: A frequency-domain approach to watermarking 3D shapes. *Computer Graphics Forum 21* (2002), 373–382.

[PAB07] PELECHANO N., ALLBECK J. M., BADLER N. I.: Controlling individual agents in high-density crowd simulation. In *Proc. Symp. Computer Animation 2007* (2007), pp. 99–108.

[Per] PERLIN K.: Adventures in robot path planning. http://mrl.nyu.edu/ perlin/experiments/path/.

[PPD07] PARIS S., PETTRE J., DONIKIAN S.: Pedestrian reactive navigation for crowd simulation: a predictive approach. *Computer Graphics Forum 26* (2007), 665–675.

[Rey99] REYNOLDS C. W.: Steering behaviors for autonomous characters. In *Proc. Game Developers Conf. '99* (1999), pp. 763–782.

[Sho85] SHOEMAKE K.: Animating rotation with quaternion curves. In *Proc. Siggraph '85* (1985), pp. 245–254.

[SKG05] SUNG M., KOVAR L., GLEICHER M.: Fast and accurate goal-directed motion synthesis for crowds. In *Proc. Symp. Computer Animation 2005* (2005), pp. 291–300.

[SM00] SHI J., MALIK J.: Normalized cuts and image segmentation. *IEEE Trans. Pattern Analysis and Maching Intelligence 22* (2000), 888–905.

[SMK05] SAKUMA T., MUKAI T., KURIYAMA S.: Psychological model for animating crowded pedestrians. *Computer Animation and Virtual Worlds 16* (2005), 343–351.

[ST05] SHAO W., TERZOPOULOS D.: Autonomous pedestrians. In *Proc. Symp. Computer Animation 2005* (2005), pp. 19–28.

[Tau95] TAUBIN G.: A signal processing approach to fair surface design. In *Proc. Siggraph '95* (1995), pp. 351–358.

[TCP06] TREUILLE A., COOPER S., POPOVIĆ Z.: Continuum crowds. *ACM Trans. Graphics 25* (2006), 1160–1168.